ENVIRONMENTAL RESEARCH
LETTERS

LETTER · OPEN ACCESS

Impact of downward longwave radiative deficits on Antarctic sea-ice extent predictability during the sea ice growth period

To cite this article: Ivana Ceroveki *et al* 2022 *Environ. Res. Lett.* **17** 084008

ENVIRONMENTAL RESEARCH
LETTERS

LETTER

Impact of downward longwave radiative deficits on Antarctic sea-ice extent predictability during the sea ice growth period

Ivana Cerovečki[1,*], Rui Sun[1], David H Bromwich[2,*], Xun Zou[1,2], Matthew R Mazloff[1] and Sheng-Hung Wang[2]

[1] Scripps Institution of Oceanography, University of California, San Diego, La Jolla, CA, United States of America
[2] Byrd Polar and Climate Research Center, The Ohio State University, Columbus, OH, United States of America
[*] Authors to whom any correspondence should be addressed.

E-mail: bromwich.1@osu.edu

Keywords: Antarctic subseasonal sea ice predictability, downward longwave radiation deficit, coupled modeling of the Southern Ocean

Supplementary material for this article is available online

OPEN ACCESS

RECEIVED
14 February 2022

REVISED
29 June 2022

ACCEPTED FOR PUBLICATION
30 June 2022

PUBLISHED
18 July 2022

Abstract

Forecasting Antarctic atmospheric, oceanic, and sea ice conditions on subseasonal to seasonal scales remains a major challenge. During both the freezing and melting seasons current operational ensemble forecasting systems show a systematic overestimation of the Antarctic sea-ice edge location. The skill of sea ice cover prediction is closely related to the accuracy of cloud representation in models, as the two are strongly coupled by cloud radiative forcing. In particular, surface downward longwave radiation (DLW) deficits appear to be a common shortcoming in atmospheric models over the Southern Ocean. For example, a recent comparison of ECMWF reanalysis 5th generation (ERA5) global reanalysis with the observations from McMurdo Station revealed a year-round deficit in DLW of approximately 50 Wm^{-2} in marine air masses due to model shortages in supercooled cloud liquid water. A comparison with the surface DLW radiation observations from the Ocean Observatories Initiative mooring in the South Pacific at 54.08° S, 89.67° W, for the time period January 2016–November 2018, confirms approximately 20 Wm^{-2} deficit in DLW in ERA5 well north of the sea-ice edge. Using a regional ocean model, we show that when DLW is artificially increased by 50 Wm^{-2} in the simulation driven by ERA5 atmospheric forcing, the predicted sea ice growth agrees much better with the observations. A wide variety of sensitivity tests show that the anomalously large, predicted sea-ice extent is not due to limitations in the ocean model and that by implication the cause resides with the atmospheric forcing.

1. Introduction

Reliable predictions of Antarctica's atmospheric, oceanic, and sea ice conditions are becoming increasingly important due to increased interest in this region, motivated in part by anthropogenic climate change (e.g. Kennicutt *et al* 2019). Skillful predictions on subseasonal to seasonal (S2S) scales are especially valuable tools for planning and decision makers (Merryfield *et al* 2020). However, these predictions remain a substantial challenge, even though climate models suggest that seasonal sea ice forecast skill is attainable (Holland *et al* 2013, Marchi *et al* 2019).

Several ongoing dedicated efforts are currently investigating the Antarctic sea ice predictability. The Year of Polar Prediction (YOPP) is an international campaign whose goal is to 'determine predictability and identify key sources of forecast errors in polar regions' by coordinating a period of intensive observing, modeling, and verification (Jung *et al* 2016). YOPP focuses on the development of coupled atmosphere–ocean–sea ice predictions on time scales from hours to seasons. The YOPP in the Southern Hemisphere (YOPP-SH) campaign coordinated intensive observational and modeling efforts in the Southern Ocean during the special observing period November 2018–February 2019 (Bromwich *et al* 2020). The Sea Ice Prediction Network South (SIPN South) is an international project under YOPP-SH whose goal is to assess the ability of current seasonal forecasting systems to predict Antarctic sea ice by a systematic and coordinated evaluation of seasonal sea ice forecasts (Massonnet *et al* 2018, 2019). The focus is on the summer season, which is of particular interest

due to marine traffic. The most recent results of SIPN South showed that the seasonal sea ice forecasts are not yet sufficiently accurate to be used to guide field planning or maritime route forecasting (Massonnet *et al* 2020, 2022). The S2S Prediction research project, established by the World Weather Research Programme/World Climate Research Programme, has the goal to improve forecast skills at the S2S timescale (Vitart *et al* 2017). The main deliverable of this project is the establishment of an extensive publicly available database of subseasonal (up to 60 days) forecasts from fully coupled atmosphere–ocean sea ice systems from several operational forecasting centers (Vitart *et al* 2017), and these are used here to explore the skill of current sea-ice extent predictions.

The skill of sea ice cover prediction depends strongly on different atmospheric and oceanic parameters. One of them is the accuracy of cloud representation in models, as the two are tightly coupled by cloud radiative forcing (e.g. Kay *et al* 2016, Schneider and Reusch 2016). Clouds have a strong influence on the onset, extent, intensity, and duration of surface melting and subsequent refreezing by altering the net surface radiative flux (e.g. van Tricht *et al* 2016, Scott *et al* 2017). In the Southern Ocean, climate models show a positive bias in net surface radiation in spring–summer due to weak shortwave cloud forcing, which is gradually reduced during autumn and winter (Schneider and Reusch 2016). In winter, climate models show a deficit in net longwave radiation, due to the bias in longwave cloud radiative effects (Schneider and Reusch 2016). However, despite the importance of accurate cloud representation in models, there is limited knowledge concerning the microphysical structure and radiative effects of clouds over the Southern Ocean, Antarctic sea ice, and Antarctic continental ice (e.g. Scott and Lubin 2016, McFarquhar *et al* 2021).

In this work, we consider the sea ice growing season, when the shortwave radiation around Antarctica is limited, and the shortwave radiation bias due to weak shortwave cloud forcing is minimal (Schneider and Reusch 2016). We focus on the surface downward longwave radiation (DLW), which has significant implications for the resilience of ice surfaces in the polar regions (e.g. Zou *et al* 2021). Silber *et al* (2019) examined the DLW measured at McMurdo Station, Antarctica during the atmospheric radiation measurement (ARM) West Antarctic Radiation Experiment (Lubin *et al* 2020), February–November 2016. The observations were stratified into clear, ice clouds, thin clouds containing liquid water, and thick clouds with liquid water that act as black bodies. For the observed clear sky and ice cloud cases, the ECMWF reanalysis 5th generation (ERA5) DLW biases were close to zero on average. For the observed liquid water clouds that were probably mixed phase, the ERA5 DLW values were smaller than observed by up to 100 Wm^{-2} with an average negative bias of around 50 Wm^{-2}. As a result, surface temperatures were cold biased. Similarly, Wang *et al* (2020) compared ERA5 DLW values with DLW measurements taken during austral summer (DJF) ship cruises to Antarctica primarily in the eastern hemisphere. Negative ERA5 DLW biases of 30–40 Wm^{-2} were found for open-ocean conditions. We hypothesize that these marine cloud DLW biases in ERA5 are representative of those that occur in atmospheric models near the Antarctic ice edge where no direct observations are available and where oceanic air masses are dominant.

A cold surface bias has also been identified by Zampieri *et al* (2019). Using the S2S Prediction research project database, Zampieri *et al* (2019) carried out the first thorough assessment of the skill of current operational ensemble forecasting systems in predicting the Antarctic sea ice edge on subseasonal timescales. Analysis of the 12 year reforecast period (1999–2011) showed that only one of six forecast systems, the European Centre for Medium-Range Weather Forecasts (ECMWFs), outperformed persistence and climatology benchmarks for lead times from about 5–30 days. On average, the other systems performed more poorly than either of these two benchmarks at any lead time considered. During both the freezing and the melting season sea ice biases were caused by a systematic overestimation of the sea-ice edge location, which was too far northward in the predictions. Zampieri *et al* (2019) hypothesized that the bias in the freezing season could be caused by a misrepresentation of thermodynamic processes in the coupled models, causing the oceanic surface to cool and freeze too rapidly. They attributed the bias in the melting season to an initial overestimation of the sea-ice thickness, which delays the onset of melting and retreat of the ice edge in spring. However, the S2S database used in Zampieri *et al* (2019) did not provide the necessary data for authors to test these hypotheses. A similar scenario was proposed by Li *et al* (2017). They suggested that including falling-snow radiative effects in models can improve simulations of Antarctic sea-ice, reducing the mismatch with the observations. When the radiative effects of falling snow were included in the community Earth system model version 1 (CESM1) model, they reduced model-observation discrepancy in sea-ice area at 50–70° S by 39% in summer and 55% in winter, mainly because increased wintertime longwave heating restricts sea-ice growth and so reduces summer albedo. Snow radiative effects reduced the winter (June–August) DLW negative bias at 58–70° S relative to the observations from 30 Wm^{-2} down to 10 Wm^{-2}.

Motivated by the recent results of Silber *et al* (2019), Li *et al* (2017) and Zampieri *et al* (2019), the goal of this study is to better understand and quantify the errors that rapidly degrade the skill of S2S forecasts for sea ice around Antarctica during the freezing season.

We compare the available DLW radiation observations from the high latitude Southern Hemisphere ocean to the commonly used ERA5 estimates. In agreement with Silber *et al* (2019), we find that ERA5 underestimates DLW radiation. Using our regional ocean sea ice model and coupled ocean–atmosphere model we perform sensitivity analyses of the sea ice evolution during the freezing season to explore potential sources of biases of sea ice forecasts, including the underestimate of the DLW radiation.

The manuscript is organized as follows. In section 2, we describe the S2S database, our regional model setups, and the observations used in this work. The observations of DLW radiation from the southernmost long-term, open ocean flux mooring are presented in section 3. The sea ice extent predictability during the sea ice formation season is analyzed considering a case study from May 2018, first using data from S2S database. The potential sources of such identified sea ice forecast biases are further explored using our regional model simulations (section 4). These include numerous sensitivity analyses, the results of some are also provided in the appendix. Summary and conclusions are provided in section 5.

2. Tools and methods

2.1. Data

We consider the ensemble sea ice and atmospheric forecasts from the four forecasting systems that employ a dynamical sea ice model: ECMWF, Environment and Climate Change Canada (ECCC), UK Met Office (UKMO), and Météo-France (MF), available from the S2S database (Vitart *et al* 2017). The operational model forecasts of the mean sea level pressure (MSLP) are provided instantaneously at midnight (00 UTC), and the sea ice concentration forecast is provided as a daily-average. The MSLP forecasts were verified against ECMWF ERA5 atmospheric reanalysis with 0.25° horizontal resolution (Hersbach *et al* 2020), and the sea ice concentration was verified using the NSIDC-0081 product derived from satellite observations (Maslanik and Stroeve 1999).

2.2. Regional model

We use a regional Southern Ocean setup of the Massachusetts Institute of Technology (MIT) general ocean circulation model (MITgcm), Marshall *et al* (1997), that we run either uncoupled or coupled with the atmospheric Polar Weather Research and Forecasting (Polar WRF) model (e.g. Bromwich *et al* 2013, Deb *et al* 2016, 2018) to simulate the evolution of Antarctic sea ice (figure 1). This coupled model builds on the Scripps–KAUST Regional Integrated Prediction System (SKRIPS, Sun *et al* 2019). The coupler uses the Earth System Modeling Framework (ESMF). The setups of the Southern Ocean models are detailed in the appendix (figure S1).

The stand-alone MITgcm ocean model is implemented using a horizontal grid with 960 × 960 points (the grid spacing of approximately 10 km) and a polar stereographic projection, to match the atmospheric Polar WRF in the coupled system. The model resolution is similar or higher than those used in the S2S forecasts database, ensuring that all the processes resolved in the current S2S efforts are resolved in the MITgcm model. The MITgcm sea-ice model (Losch *et al* 2010) does have a relatively simple thermodynamics component, being based on the 0-layer formulation of Semtner (1976), but has numerous important modifications to simulate the most important ice growth processes (Fenty and Heimbach 2013). This model has been used extensively to simulate the sea ice in the Arctic and Antarctica (e.g. Fenty *et al* 2017).

2.3. DLW radiation observations

To quantify the inferred DLW negative biases in ERA5 close to the sea-ice edge we examine observations from the OOI Southern Ocean mooring, located in the southeast Pacific, to the west of the southern tip of Chile (54.08° S, 89.67° W). This is the farthest south long-term, open ocean flux mooring ever deployed (Ogle *et al* 2018). The mooring was maintained from February 2015 until January 2020, when it was removed. We additionally examine high quality DLW observations from the Antarctic coast adjacent to the Weddell Sea (figure S2).

The OOI Apex surface mooring (OOI site ID GS01SUMO) was mounted with the Bulk Meteorology Instrument Package (METBK, with the ID GS01SUMO-SBD12-06-METBKA000), that included duplicate Star Engineering ASIMET packages (OOI data streams METBKl1 and METBK12). These provided 1 min averaged measurements of downwelling longwave irradiance, measured by an Eppley Precision Infrared Radiometer sensor, which was part of the ASIMET longwave radiation module. The instrument has the range 0–700 Wm^{-2}, resolution 0.1 Wm^{-2} and a drift (post vs. pre calibration after one year) of 2 Wm^{-2} (Colbo and Weller 2009). The uncertainty of the instrument is about 4 Wm^{-2} for daily averages (Colbo and Weller 2009). Observations are available from the four overlapping deployments: 18 February 2015–27 December 2015, 14 December 2015–12 December 2016, 25 November 2016–9 December 2018, and 4 December 2018–20 January 2020 (figure 2(a)). However, there are significant gaps in the mooring observations. Upon mooring recovery after the second deployment, damage to some components of the surface buoy was reported, including to the METBK. During the third deployment (25 November 2016–9 December 2018), the DLW observations from the two packages showed an offset of approximately 5 Wm^{-2}. The offset was reported in the documentation, provided as guidance to prospective researchers, available

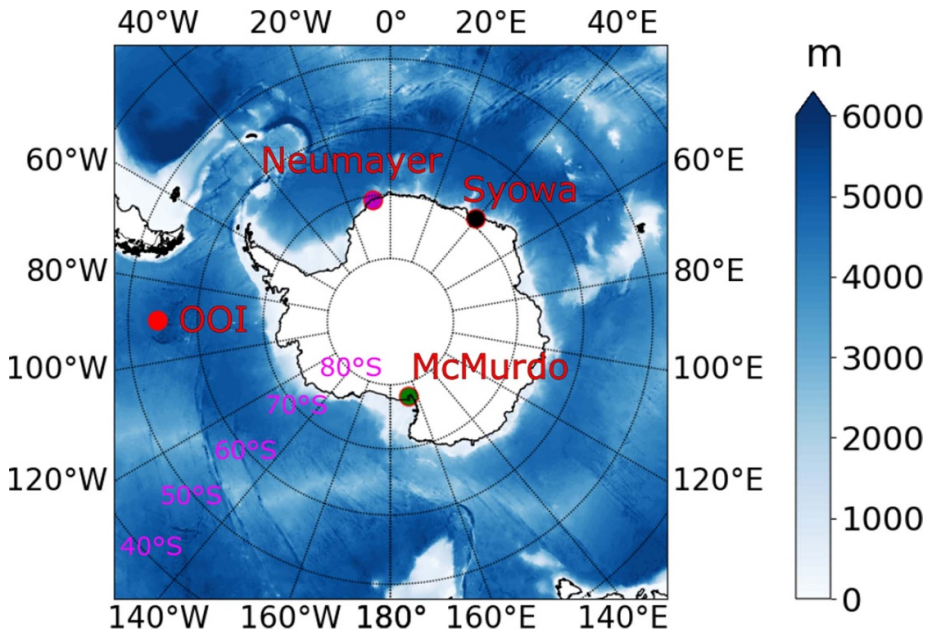

Figure 1. The ocean model domain and (color) bathymetry, and the locations of the observations considered in this study: the Ocean Observatories Initiative (OOI) mooring, Neumayer station, Syowa station, and McMurdo station.

from https://ooinet.oceanobservatories.org/. Following the guidance from the documentation, we increased the DLW radiation measured by package 12 by 5 Wm^{-2} during the time period of the third deployment.

3. DLW radiation deficit estimates

The 1 min averaged measurements of DLW radiation from the OOI mooring were first time-averaged to hourly means. The observations from the first deployment 18 February 2015–27 December 2015 were not considered in our analysis because of the significant data gaps (figures 2(a) and (b)). For the other three deployments we additionally omitted the time periods of mooring recovery and redeployment, thus restricting our analysis to the three time periods indicated in figure 2(b): period one from 1 January 2016 to 7 November 2016, period two from 14 December 2016 to 12 November 2018, and period three from 7 December 2018 to 20 January 2020. The average difference between the hourly DLW radiation from the two meteorological packages was -4.3 Wm^{-2} in period one, 0.6 Wm^{-2} in period two (after the bias correction discussed above) and -0.8 Wm^{-2} in period three (figure 2(b)). Hereafter we consider the average of the observations from the two meteorological packages. During all three time periods, ERA5 underestimated the DLW radiation compared to the observations, with the difference between the hourly means of -18.7 Wm^{-2}, -21.4 Wm^{-2} and -7.3 Wm^{-2} respectively (figure 2(d)).

Comparison of the monthly mean of the average of the two sets of OOI mooring observations with monthly mean reanalyses gives the systematic differences in DLW estimates. For time periods one and two (January 2016–November 2018) the difference between ERA5 DLW radiation and mooring observations is relatively constant and equals -17.2 Wm^{-2} (figure 3). We omit period three from figure 3 because the OOI DLW observations show a sudden jump at the start of this period. Such a jump is not evident in the reanalysis data and we were unable to find information about a potential offset during the fourth deployment (i.e. period three). We also assessed ERA-Interim and National Centers for Environmental Prediction (NCEP)-National Center for Atmospheric Research (NCAR). Reanalysis 1 monthly means of DLW, and found they were both biased low compared to the observations (-12.9 and -28.3, respectively, figure 3). A negative bias in monthly mean DLW was also shown at both coastal Antarctic Baseline Surface Radiation Network (BSRN) stations close to the Weddell Sea (Neumayer and Syowa), for the period 2016–2020, with a range from -2 to -19 Wm^{-2}. The negative bias has an annual cycle with a maximum DJF and a minimum around August (figure S2; more details in appendix). Compared to the OOI mooring observations, the BSRN stations are at a higher latitude at the edge of Antarctica and suggest a smaller negative bias in ERA5. The negative bias in ERA5 is conjectured to maximize around 50 Wm^{-2} at the sea-ice edge, a region that is impacted much more frequently by marine air masses. Our results suggest that a significant deficit in DLW is a common problem in atmospheric models over the Southern Ocean. In particular, ERA5 has a DLW deficit on the order of 20 Wm^{-2} over the open ocean well north of the sea-ice edge.

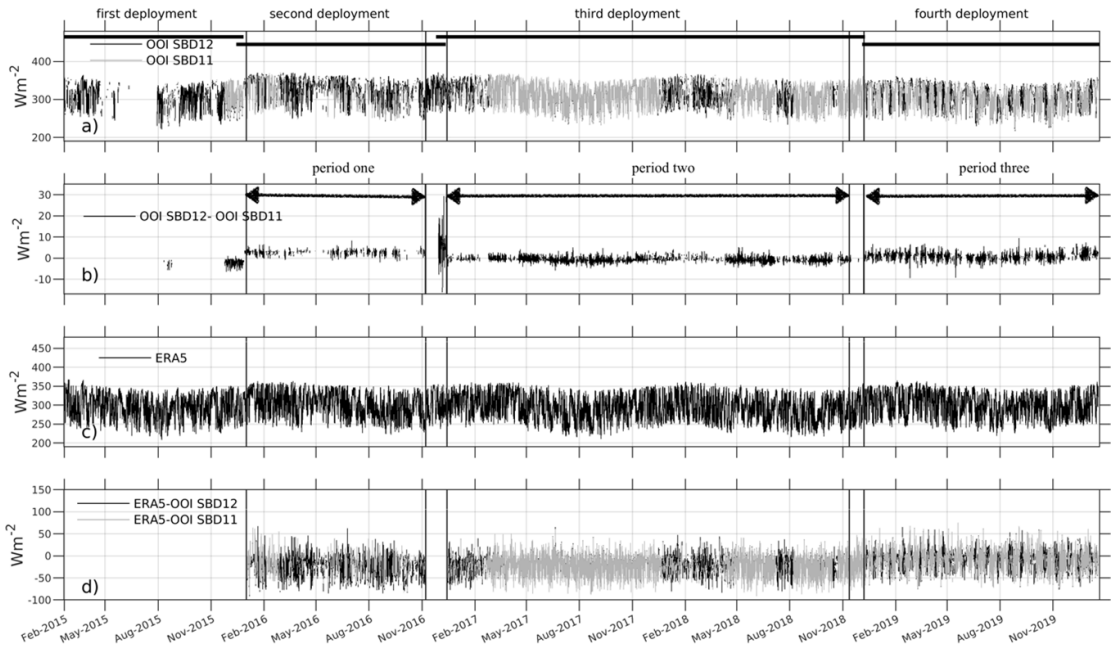

Figure 2. (a) Hourly averaged DLW radiation obtained from the 1 min averaged measurements by the two meteorological packages (OOI SBD12 in black and OOI SBD11 in gray) that were mounted on the OOI mooring; thick black horizontal lines indicate the time periods of the four overlapping mooring deployments, (b) the difference between the two sets of the DLW observations shown in panel a, shown as OOI SBD12 minus OOI SBD11 observations; the three time periods considered in our analysis are indicated both by arrows and by vertical lines (latter shown in all the panels), (c) ERA5 hourly averaged DLW radiation and (d) the difference between ERA5 DLW radiation shown in panel c and (black) OOI SBD12 and (gray) OOI SBD11. All in Wm^{-2}.

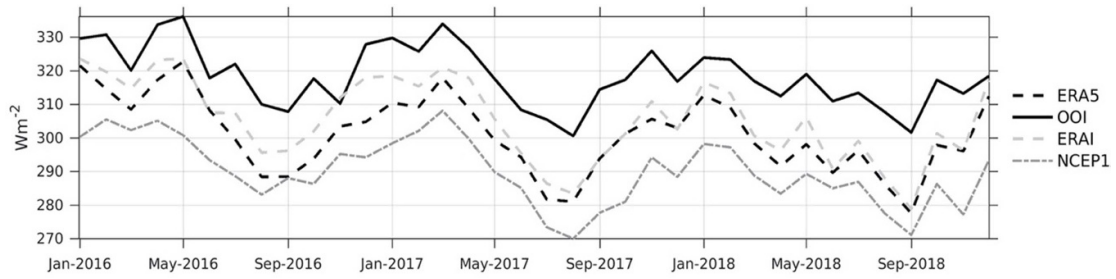

Figure 3. The monthly mean DLW radiation for period January 2016–November 2018: (black solid) the average of the two sets of OOI mooring observations, (black dashed) ERA5, (light gray dashed) ERA-Interim (ERAI), and (darker gray dashed) NCEP-NCAR Reanalysis 1 (NCEP1).

4. The May 2018 case study

4.1. Sea ice overestimation in May 2018 in the S2S forecasts

The predictive skill of operational S2S ensemble forecast systems during the sea ice growth season was examined by considering a case study from May 2018, which falls within the YOPP period (2017–2019). In 2018, the Antarctic continent was considerably warmer than on average, with a record-low sea-ice extent in the Weddell and Ross Seas (Scambos and Stammerjohn 2019). From austral autumn to early winter (March to June), low pressure anomalies over the Antarctic Peninsula and high pressure anomalies over the continental interior caused widespread warm temperatures, decreasing the circumpolar sea-ice extent well below average (Scambos and Stammerjohn 2019). Despite these extreme seasonal and regional climate anomalies in the year 2018, we found that the sea ice forecast biases diagnosed in May of 2018 were representative of other years as well (figures S3 and S4). In the text that follows, we predominantly show examples from the ECMWF forecasting system, which demonstrated the highest sea ice forecasting skill in the Zampieri *et al* (2019) analysis.

We consider the atmosphere-sea ice forecast by the ECMWF forecasting system initialized on 10 May 2018. On the day the forecast was initialized, there was a close agreement between the ECMWF and ERA5 MSLP, and the standard deviation between the 20 ECMWF ensemble members was negligible (figures 4(a), (d) and (g)). The ECMWF sea-ice edge extended somewhat further north than in the NSIDC

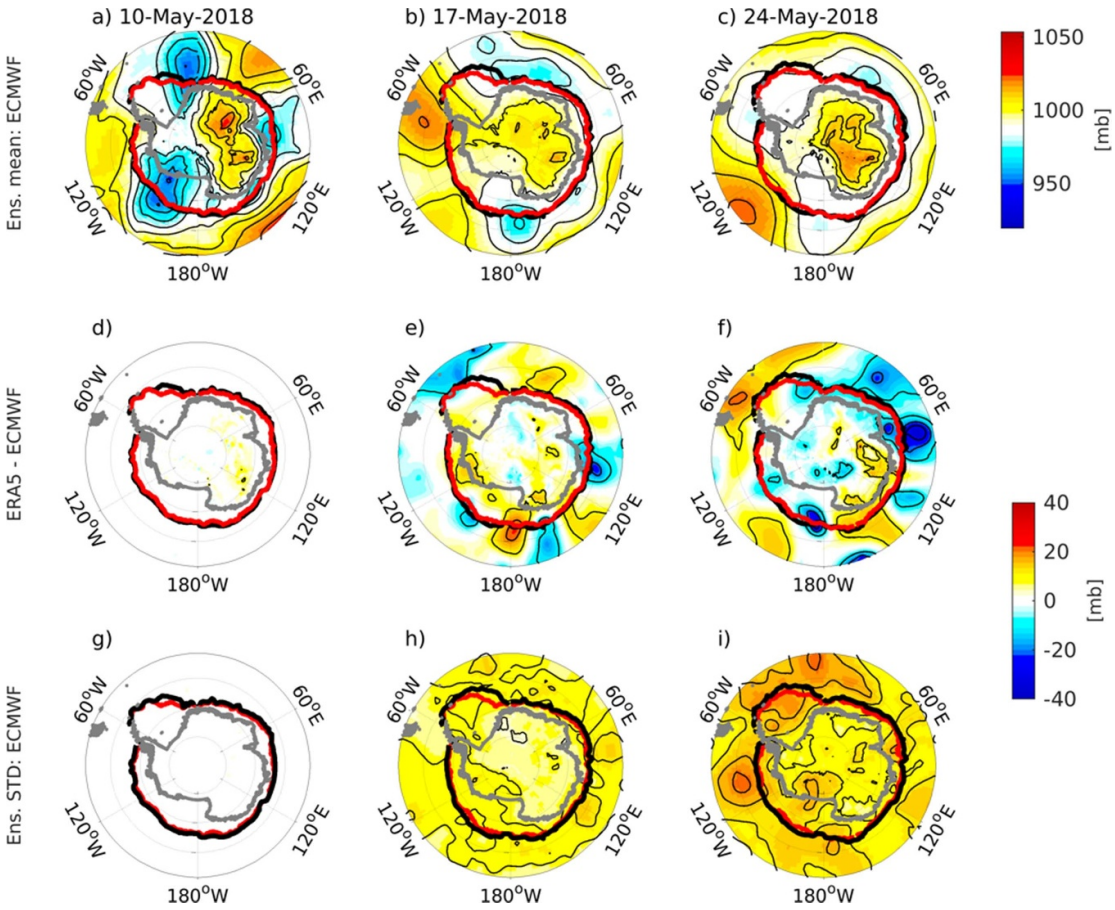

Figure 4. (Top, color) The ECMWF operational model forecast of the instantaneous MSLP at midnight (00 UTC), (a) initiated on 10 May 2018, (b) one week forecast, and (c) the two-week forecast. In all panels (a)–(i), the daily-average sea-ice edge (defined by 15% concentration) from the ensemble mean (heavy black line) is compared to the NSIDC-0081 observations (heavy red line); (d)–(f) the difference between the hourly averaged MSLP (00–01 UTC) from ERA5 reanalysis and the instantaneous ECMWF MSLP shown in panels (a)–(c); (g)–(i) (color) the standard deviation of 20 ensemble members whose average is shown in panels (a)–(c). Contour interval is (a)–(f) 10 mb and (g)–(i) 4 mb. In (d)–(f), zero contour has been omitted.

observations in the eastern Weddell Sea (figures 4(d) and 5(a)). Comparison with the ERA5 reanalysis and the NSIDC observations shows a degradation of both the ECMWF atmospheric and sea ice forecast skill after approximately one week, when the MSLP pattern was misrepresented by ECMWF (figures 4(b) and (e)). The forecast skill further decreased in the two-week forecast (figures 4(c) and (f)). The mismatch between the ECMWF one week and two-week MSLP forecasts and the corresponding ERA5 estimates was often larger than the MSLP ensemble spread (figures 4(e), (f), (h) and (i)).

The sea-ice edge estimates (defined by 15% sea-ice concentration contour) from four forecast systems available from S2S dataset that were initialized on 10 May 2018 show large differences already at the time forecasts were initialized (figures 5(a) and 6(a)), especially in the eastern Weddell Sea (figure 5(a)). Similarly, the largest bias in a two-week forecast, as well as intermodel spread, was in the eastern Weddell Sea (figures 5(a) and (b)), in agreement with Massonnet *et al* (2020). Consistent with Zampieri *et al* (2019), most systems overestimated the forecasted sea ice growth, so that the sea ice edge extended too far north (figure 5(b)). Only the ECCC forecast greatly underestimated the sea-ice extent in the eastern Weddell Sea (figure 5(b)).

4.2. Analysis of the sea ice bias in May 2018 using the regional model

The sea ice bias identified in the S2S forecasts is further examined using uncoupled and coupled MITgcm regional model simulations. The sea ice evolution during the time period from 10 May to 1 June was compared to the NSIDC observations, and to the ensemble mean forecasts from the four operational models from S2S database that were initialized on 10 May 2018 (and considered in figure 5). The common feature of the time evolution of the circumpolar sea-ice area estimates (defined as area enclosed with 15% sea-ice concentration contour) from four operational models, uncoupled and coupled MITgcm regional model simulations is too fast sea ice growth (figure 6(a)).

The forecasts given by the four operational systems show large differences, with biases that even

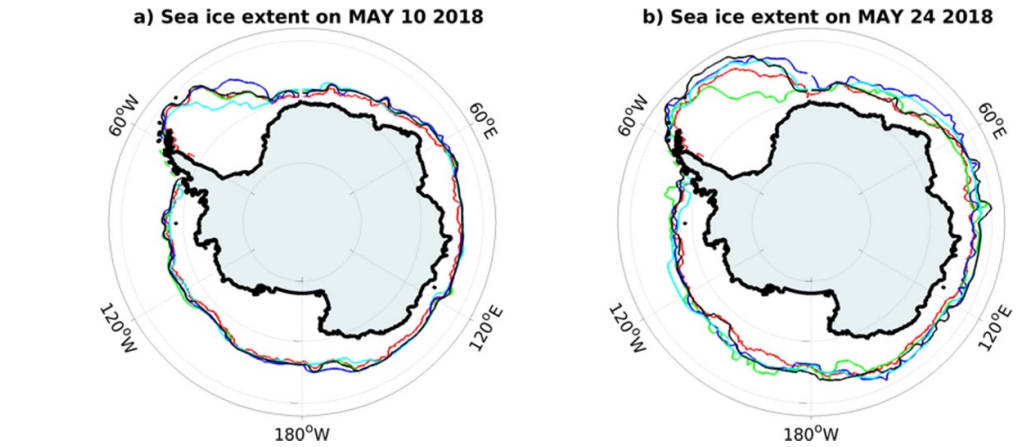

Figure 5. The sea-ice extent, shown by 15% sea-ice concentration contour, from the observations (red, NSIDC-0081; Maslanik and Stroeve 1999), and from control forecasts from four forecast systems from S2S database: (green) ECCC, (blue) ECMWF, (black) UK Met Office, and (light blue) Météo-France model (a) on 10 May 2018 when forecasts were initialized, and (b) a two-week forecast.

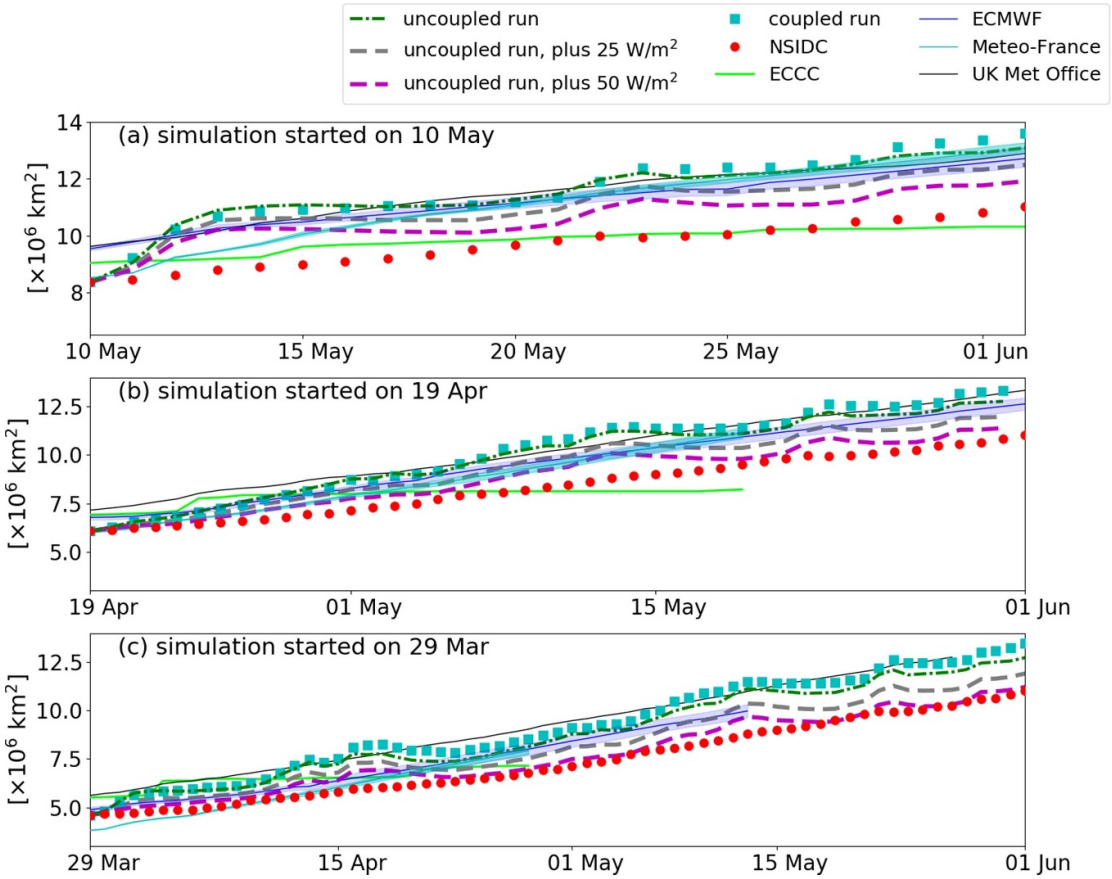

Figure 6. The circumpolar sea-ice area (enclosed by 15% sea-ice concentration contour) obtained from the regional MITgcm numerical model (green dot-dashed) uncoupled simulation, (cyan squares) coupled simulation, (gray dashed) uncoupled simulation with an artificial increase of DLW by 25 Wm^{-2}, (magenta dashed) uncoupled simulation with an artificial increase of DLW by 50 Wm^{-2}, (red dots) NSIDC observations, and the four forecast systems available from S2S database: (green) ECCC, (blue) ECMWF, (black) UK Met Office, and (light blue) Météo-France model, for the simulations and S2S forecasts initialized on (a) 10 May, (b) 19 April and (c) 29 March 2018. For the S2S forecasts, the solid line indicates the ensemble mean, and the shaded area indicates the ensemble mean plus/minus one standard deviation.

differ in sign (figure 6). On the day forecasts were initialized, the ECCC and MF circumpolar sea-ice area were closer to the NSIDC observations than those from ECMWF and UKMO, which showed a positive bias (figure 6(a)). During the entire time period considered, the mean bias between the circumpolar sea-ice area estimates by ECCC and the observations is smaller than for the other three systems. This

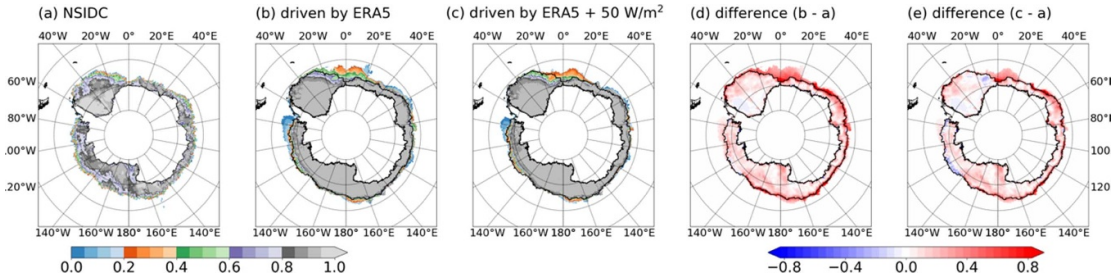

Figure 7. (Color) the sea-ice fraction on 24 May 2018 (a) from the NSIDC data, and (b), (c) from the uncoupled MITgcm model simulation initialized on 10 May 2018, driven by (b) ERA5 and (c) ERA5 with an artificial increase of DLW radiation by 50 Wm^{-2}. Panels (d) and (e) show the difference between the two simulations and NSIDC data, as indicated in the title. The black contours indicate the sea-ice extent from NSIDC data.

Table 1. A comparison of the sea ice growth rate estimates from the regional model simulations with the NSIDC observations. The sea ice growth rate is calculated based on the linear regression of the sea ice extent area.

	Uncoupled model	Coupled model	Uncoupled model + 50 Wm^{-2}	NSIDC data
Initialized on 10 May 2018	1.67×10^5 m^2 d^{-1}	1.88×10^5 m^2 d^{-1}	1.25×10^5 m^2 d^{-1}	1.15×10^5 m^2 d^{-1}
Initialized on 19 April 2018	1.60×10^5 m^2 d^{-1}	1.75×10^5 m^2 d^{-1}	1.30×10^5 m^2 d^{-1}	1.19×10^5 m^2 d^{-1}
Initialized on 29 March 2018	1.22×10^5 m^2 d^{-1}	1.30×10^5 m^2 d^{-1}	1.02×10^5 m^2 d^{-1}	1.01×10^5 m^2 d^{-1}

primarily results from the cancellation of biases of opposing signs, as is evident in figure 5(b). Analysis of the integrated ice area error (figure S5(a)) reveals that, in consistency with Zampieri *et al* (2019), ECMWF shows the most skill of the S2S forecasting systems.

Similar to the four forecasting systems from S2S datasets, the uncoupled MITgcm model simulations overestimated the sea ice growth (figure 6(a)), and had slightly lower skill than the ECMWF forecasts (figure S5(a)). Figures 7(b) and (d) show that the uncoupled MITgcm model has a large bias in the eastern Weddell Sea. The sea ice growth was also overestimated by the coupled model simulations (figure 6(a)). Li *et al* (2017) showed that including the radiative effects of precipitating ice (falling snow) improved climate model simulations of Antarctic sea ice. These effects were parameterized in the Morrison microphysics scheme in the coupled run, but not in the uncoupled run. While the DLW radiation in the coupled model was higher by 10–20 Wm^{-2} in the region covered by sea ice, the sea ice growth was still too fast, as the net surface heat loss Qnet in the coupled run has not been uniformly reduced relative to the uncoupled run. In our case both the coupled and uncoupled model simulations overestimated the sea-ice growth (coupled model: 1.88×10^5 m^2 d^{-1}; uncoupled model: 1.67×10^5 m^2 d^{-1}) compared with NSIDC (1.15×10^5 m^2 d^{-1}) after 21 days (table 1), as was seen in the forecasts from ECMWF, UK Met, and MF.

Motivated by a diagnosed deficit in ERA5 DLW radiation, estimated by comparison with the observations, we additionally ran an uncoupled simulation in which the DLW radiation was artificially increased by 25 Wm^{-2} south of 60° S. While this greatly improved the skill of the simulation (figure S5(a)) and did reduce the mismatch between the modeled (1.45×10^5 m^2 d^{-1}) and the observed sea ice extent growth (figure 6(a)), it was still necessary to artificially increase the DLW by 50 Wm^{-2} south of 60° S to further reduce the mean sea ice extent area bias (figures 6(a) and 7(c), table 1). The strongest sea ice concentration decrease by this artificial increase of DLW was in the eastern Weddell Sea (figure 7(c)). However, compared to the observations, the model still overestimated sea ice area growth (1.25×10^5 m^2 d^{-1}, table 1).

The result that a deficit of DLW may be degrading sea ice forecast skill agrees with the implications of Silber *et al* (2019), who estimated a year-round deficit in DLW at McMurdo Station of approximately 50 Wm^{-2} in marine air masses in the ERA5 reanalysis. An artificial increase in DLW by 50 Wm^{-2} decreased the surface ocean heat loss by approximately 40–50 Wm^{-2} south of 60° S (figure S6), reducing the model sea ice growth, and bringing it closer to the observations (figure 6(a)). Very similar results were obtained for years 2016 and 2017 (figure S3), demonstrating that 2018 findings are representative of other years. The agreement between the modeled and the observed sea ice extent was even better for the simulations initialized before 10 May, as discussed in the next section.

4.3. Sensitivity analysis of the ocean and sea ice model

In order to examine whether the bias in sea ice growth in our hindcast model simulations could be reduced by changing the representation of the most relevant sea ice and oceanic conditions, we performed

a series of sensitivity analyses. Because the ocean acts as an integrator of the atmospheric forcing, we first examined the sensitivity of sea ice extent to the ocean model initialization date. We ran two additional uncoupled model simulations initiated earlier in the sea ice growth season, on the same days as the operational models' forecasts available from the S2S database (29 March and 19 April 2018; figures 6(b), (c) and S5(b), (c)). Although the sea ice growth was initially somewhat slower than in the simulation initialized on 10 May 2018, by 1 Jun 2018, the sea ice growth was overestimated in all three simulations (19 April from uncoupled model: 1.60×10^5 m^2 d^{-1}, from NSIDC: 1.19×10^5 m^2 d^{-1}; 29 Mar from uncoupled model: 1.22×10^5 m^2 d^{-1}, from NSIDC: 1.01×10^5 m^2 d^{-1}). When we artificially increased the DLW radiation by 50 Wm^{-2}, the model sea-ice area from all three simulations was generally consistent with the NSIDC data (table 1), especially for the two simulations initialized before 10 May 2018 (19 April from model: 1.30×10^5 m^2 d^{-1}, from NSIDC: 1.19×10^5 m^2 d^{-1}; 29 March from model: 1.02×10^5 m^2 d^{-1}, from NSIDC: 1.01×10^5 m^2 d^{-1}). This is likely because more heat remains in the ocean with a more prolonged DLW increase, which helps to slow subsequent sea ice growth. Very similar results were obtained for the years 2016 and 2017 (figure S4), again confirming the generality of the analysis for 2018.

We also examined whether changing the commonly used definition of sea ice extent given by the 15% sea-ice concentration would reduce the discrepancy. However, using sea ice extent defined by the 30% and 50% sea-ice concentration contours did not reduce the mismatch between the model and the observations (figure S8(a)). When we artificially increased the DLW radiation by 50 Wm^{-2} in our uncoupled model simulation, the comparison was much better for all three definitions of sea-ice extent (figure S8(b)).

Other extensive sensitivity analyses were carried out, including turning off sea ice dynamics and changing the lead closing parameter h_0 in the sea ice model. We also did runs changing the ocean model vertical diffusion coefficients and also the initial conditions. However, the results of these experiments, most of which are presented in the appendix, all demonstrated minimal sensitivity of the simulated sea-ice growth to parameters other than the DLW radiation.

5. Summary and conclusions

The prediction of Southern Ocean clouds and their impact on the downward radiative fluxes plays a major role in sea ice predictive skill (e.g. Kay *et al* 2016). Recent observationally based findings showed that the atmospheric model biases in the representation of mixed-phase cloud microphysical processes can yield strong cold surface bias around Antarctica (Silber *et al* 2019). The cold bias, and a systematic overestimation of the sea-ice edge location, was also diagnosed in commonly used forecast systems, whose output is available from the S2S database (Zampieri *et al* 2019). These recent findings motivated us to examine causes for loss of predictability in the Antarctic sea ice subseasonal forecast during the sea-ice expansion season, when shortwave radiation in the high latitude Southern Ocean is small. During this time a spring–summer positive shortwave radiation bias due to weak shortwave cloud forcing is minimal (Schneider and Reusch 2016). We thus focus on the impact of a DLW radiation deficit near the Antarctic sea ice edge, where no direct observations are available and where oceanic air masses are dominant.

Because of the lack of DLW observations from the marginal ice zone, we examined the DLW observations representative of the marine air masses. The monthly mean mooring observations from the farthest south, long-term, open-ocean flux mooring ever deployed, located in the southeast Pacific (Ogle *et al* 2018), showed a relatively constant ERA5 DLW radiation bias of approximately -17.2 Wm^{-2} during the time period January 2016–November 2018. The uncertainty of the instrument is about 4 Wm^{-2} for daily averages (Colbo and Weller 2009). Similarly, the high quality DLW observations from Neumayer and Syowa stations on the Antarctic coast adjacent to the Weddell Sea region with large forecast sea-ice differences showed negative ERA5 DLW biases of 5 and 20 Wm^{-2}, respectively. These biases are comparable to those diagnosed at McMurdo Station, Antarctica, by Silber *et al* (2019) for marine air masses. A comparison with the observations thus suggests that ERA5 DLW radiation underestimate is of the order of 20–50 Wm^{-2}.

We further examine the causes of sea ice growth biases, focusing on one case study, in May 2018. We consider output of four forecasting systems initialized on 10 May 2018, available from S2S database, combined with dedicated simulations using our regional numerical ocean model. Both show loss of atmospheric and sea ice predictability after approximately one week. Three of the four forecasting systems overestimated the sea ice growth, so that the sea ice edge extended too far north by the end of May. Such an overestimate in sea ice growth by S2S forecast systems is in agreement with the results of Zampieri *et al* (2019).

Similar to S2S forecasts, the uncoupled model simulation forced by ERA5 fields, and the fully coupled simulation, both initialized on 10 May 2018, overestimated the sea ice growth, especially in the Weddell Sea (figures 6 and 7). Motivated by the observational results, in order to reduce the mismatch between the modeled and the observed sea ice extent, we artificially increased the DLW by 50 Wm^{-2} south of 60° S. This decreased the surface ocean heat loss by

approximately 40–50 Wm^{-2}, reducing the uncoupled model sea ice growth rate from 1.67 $\times$ 10^5 m^2 d^{-1} to 1.25 $\times$ 10^5 m^2 d^{-1}, which is much closer to the NSIDC estimate of 1.15 $\times$ 10^5 m^2 d^{-1} (table 1). We ran two more uncoupled model simulations initialized earlier in the sea-ice growth season (on 29 March and 19 April 2018). Although the sea ice growth was initially somewhat slower than in the simulation that started on 10 May, by 1 June 2018 all the simulations similarly overestimated the sea ice growth. Artificially increasing the DLW radiation by 50 Wm^{-2} in the uncoupled model simulation significantly reduced the bias for all three simulations, especially for the two simulations initialized before 10 May 2018 (19 April and 29 March, shown in table 1). This is likely because less ocean cooling occurs in response to a more prolonged DLW increase, slowing the sea ice growth. Similar sensitivity analyses carried out for the other years gave consistent results (shown in the appendix).

The aim of other sensitivity analyses was to determine whether the bias in sea ice growth in our hindcast model simulations could be reduced by changing the representation of the most relevant sea ice and oceanic conditions. Among other tests, we investigated the sensitivity of sea ice growth to the vertical diffusion coefficient used in the ocean model, and to the lead closing parameter h_0 used in the sea ice model. Despite the importance of vertical mixing in governing the upper ocean heat content, the sea ice growth was insensitive to changes in the vertical mixing coefficient, unless we used an unphysically high value. The lead closing parameter h_0 strongly governs the vertical and horizontal sea ice growth. However, the sea ice growth in the MITgcm was not very sensitive to the wide range of h_0 values tested, and in all the cases the sea ice was growing too fast compared to the observations. Since the sea ice fraction in the marginal ice zone in the model was higher than in the observations, we also examined whether changing the commonly used definition of sea ice extent given by the 15% sea-ice concentration contour would reduce the mismatch between the sea ice extent from our model simulation and the observations. We used the 30% and 50% sea-ice concentration contour to define the sea ice edge, and in all cases the diagnosed sea ice growth in our uncoupled model simulation was faster than in the observations. When we artificially increased the DLW radiation by 50 Wm^{-2}, the comparison with the observations was much better for all three definitions of sea-ice extent. We finally examined the sensitivity of sea-ice growth to the model sea-ice dynamics and the albedo. Neither change substantially slowed the sea-ice growth. The effects of changing the albedo were small as the shortwave radiation in the high latitude Southern Ocean is very small in winter. The importance of thermodynamics, rather than sea-ice dynamics, is in agreement with Zampieri *et al* (2019). The sea ice growth was also found to not be sensitive to modest initial perturbations of the ocean surface temperature and salinity. Thus, the sensitivity analysis showed that changing these ocean and sea ice model parameters can not substantially reduce the overestimation of the sea-ice. A caveat in this study is that the sea ice model used does have simplified dynamics and thermodynamics. Nevertheless, our extensive tests suggest that the ocean-sea ice model is not responsible for the excessive sea-ice growth, and by implication the issue is inferred to reside with the atmospheric forcing. The deficit in DLW radiation is a common feature of atmospheric models used for weather prediction to climate change projections and is the likely cause of the overestimated Antarctic sea ice edge documented here.

Our results suggest that in this Antarctic region ERA5 may underestimate DLW by up to 50 Wm^{-2} during the sea ice growth period. The bias may even be larger for other reanalyses such as NCEP-NCAR Reanalysis 1. A dedicated effort to measure the energy budget at the marginal ice zone throughout the transitional sea ice growing season would yield the necessary data to identify the cause of these model biases and improve Antarctic sea ice predictability.

Data availability statement

In this work we used data from the S2S database. S2S is a joint initiative of the World Weather Research Programme (WWRP) and the World Climate Research Programme (WCRP). The original S2S database is hosted at ECMWF as an extension of the TIGGE database. ERA5 Reanalysis (0.25 Degree Latitude-Longitude Grid), generated by European Centre for Medium-Range Weather Forecasts (2019), are available from Research Data Archive at the National Center for Atmospheric Research, Computational and Information Systems Laboratory, https://doi.org/10.5065/BH6N-5N20. The NSIDC data are downloaded from https://nsidc.org/data/NSIDC-0081/versions/1. The simulation results are available at https://doi.org/10.5281/zenodo.5899938. The mooring observations used in this work are available from the NSF Ocean Observatories Initiative Data Portal, http://ooinet.oceanobservatories.org. The observations of the DLW, obtained from the Bulk Meteorology Instrument Package, are available from https://ooinet.oceanobservatories.org/data_access/?search=GS01SUMO-SBD11-06-METBKA000 and https://ooinet.oceanobservatories.org/data_access/?search=GS01SUMO-SBD12-06-METBKA000. The Ocean Observatories Initiative is a major facility fully funded by the National Science Foundation, under Cooperative Agreement No. 1743430.

The data that support the findings of this study are available upon reasonable request from the authors.

Acknowledgments

I C was supported by NASA Grant 80NSSC19K1115. D H B, X Z, and S H W were supported by NSF Grant No. 1823135. R S was supported by KAUST (King Abdullah University of Science and Technology) Grant No. OSR-2016-RPP-3268.02. M R Mazloff acknowledges support from NASA Grant Nos. 80NSSC20K1076 and 80NSSC22K0387, and NSF Grant Nos. OCE-1924388, PLR-1425989, OPP-2149501, and OPP-1936222. We also appreciate the computational resources on supercomputer Shaheen II for implementing and testing the coupled model. Contribution number C-1618 of Byrd Polar and Climate Research Center. We thank the two anonymous reviewers for their constructive comments.

Conflict of interest

The authors declare they have no conflicts of interest.

ORCID iDs

Ivana Cerovečki https://orcid.org/0000-0001-8979-9952
David H Bromwich https://orcid.org/0000-0003-4608-8071
Sheng-Hung Wang https://orcid.org/0000-0002-8057-835X

References

Bromwich D H *et al* 2020 The year of polar prediction in the Southern Hemisphere (YOPP-SH) *Bull. Am. Meteorol. Soc.* **101** E1653–76

Bromwich D H, Otieno F O, Hines K M, Manning K W and Shilo E 2013 Comprehensive evaluation of polar weather research and forecasting model performance in the Antarctic *J. Geophys. Res.* **118** 274–92

Colbo K and Weller R A 2009 Accuracy of the IMET sensor package in the subtropics *J. Atmos. Ocean. Technol.* **26** 1867–90

Deb P, Orr A, Bromwich D H, Nicolas J P, Turner J and Hosking J S 2018 Summer drivers of atmospheric variability affecting ice shelf thinning in the Amundsen sea embayment, west Antarctica *Geophys. Res. Lett.* **45** 4124–33

Deb P, Orr A, Hosking J S, Phillips T, Turner J, Bannister D, Pope J O and Colwell S 2016 An assessment of the polar weather research and forecasting (WRF) model representation of near-surface meteorological variables over West Antarctica *J. Geophys. Res.* **121** 1532–48

Fenty I and Heimbach P 2013 Coupled sea ice–ocean-state estimation in the Labrador Sea and Baffin Bay *J. Phys. Oceanogr.* **43** 884–904

Fenty I, Menemenlis D and Zhang H 2017 Global coupled sea ice-ocean state estimation *Clim. Dyn.* **49** 931–56

Hersbach H *et al* 2020 The ERA5 global reanalysis *Q. J. R. Meteorol. Soc.* **146** 1999–2049

Holland M M, Blanchard-Wrigglesworth E, Kay J and Vavrus S 2013 Initial-value predictability of Antarctic sea ice in the Community climate system model 3 *Geophys. Res. Lett.* **40** 2121–4

Jung T *et al* 2016 Advancing polar prediction capabilities on daily to seasonal time scales *Bull. Am. Meteorol. Soc.* **97** 1631–47

Kay J E, Wall C, Yettella V, Medeiros B, Hannay C, Caldwell P and Bitz C 2016 Global climate impacts of fixing the Southern Ocean shortwave radiation bias in the community earth system model (CESM) *J. Clim.* **29** 4617–36

Kennicutt M C *et al* 2019 Sustained Antarctic research: a 21st century imperative *One Earth* **1** 95–113

Li J-L F, Richardson M, Hong Y, Lee W-L, Wang Y-H, Yu J-Y, Fetzer E, Stephens G and Liu Y 2017 Improved simulation of Antarctic sea ice due to the radiative effects of falling snow *Environ. Res. Lett.* **12** 084010

Losch M, Menemenlis D, Campin J-M, Heimbach P and Hill C 2010 On the formulation of sea-ice models. Part 1: effects of different solver implementations and parameterizations *Ocean Model.* **33** 129–44

Lubin D *et al* 2020 AWARE: the atmospheric radiation measurement (ARM) West Antarctic radiation experiment *Bull. Am. Meteorol. Soc.* **101** E1069–91

Marchi S, Fichefet T, Goosse H, Zunz V, Tietsche S, Day J J and Hawkins E 2019 Reemergence of Antarctic sea ice predictability and its link to deep ocean mixing in global climate models *Clim. Dyn.* **52** 2775–97

Marshall J, Adcroft A, Hill C, Perelman L and Heisey C 1997 A finite-volume, incompressible Navier Stokes model for studies of the ocean on parallel computers *J. Geophys. Res.* **102** 5753–66

Maslanik J and Stroeve J 1999 Near-real-time DMSP SSMIS daily polar gridded sea ice concentrations, version 1 Boulder (Boulder, CO: NASA National Snow and Ice Data Center Distributed Active Archive Center) (https://doi.org/10.5067/U8C09DWVX9LM)

Massonnet F, Reid P, Lieser J L, Bitz C M, Fyfe J and Hobbs W R 2019 Assessment of summer 2018–2019 sea-ice forecasts for the Southern Ocean (Technical report) (Université catholique de Louvain) (available at: www.climate.be/users/fmasson/SIPN-South_2018-2019_postseason.pdf)

Massonnet F, Reid P, Lieser J L, Bitz C M, Fyfe J, Hobbs W and Kusahara K 2018 Assessment of February 2018 sea-ice forecasts for the Southern Ocean (Technical report) (Université catholique de Louvain) (available at: http://polarmet.osu.edu/YOPP-SH/SIPN-South_20180607.pdf)

Massonnet F, Reid P, Lieser J, Bitz C, Fyfe J and Hobbs W 2020 Assessment of summer 2019–2020 sea-ice forecasts for the Southern Ocean (Technical report) (Université catholique de Louvain) (available at: http://polarmet.osu.edu/YOPP-SH/SIPN-South_2019-2020_postseason.pdf)

Massonnet F, Reid P, Lieser J, Bitz C, Fyfe J and Hobbs W 2022 Assessment of summer 2021–2022 sea-ice forecasts for the Southern Ocean (Technical report) (Université catholique de Louvain) (available at: http://polarmet.osu.edu/YOPP-SH/SIPN-South_2021-2022_postseason.pdf)

McFarquhar G *et al* 2021 Observations of clouds, aerosols, precipitation, and surface radiation over the Southern Ocean: an overview of Capricorn, Marcus, Micre, and Socrates *Bull. Am. Meteorol. Soc.* **102** E894–928

Merryfield W J *et al* 2020 Current and emerging developments in subseasonal to decadal prediction *Bull. Am. Meteorol. Soc.* **101** E869–96

Ogle S E, Tamsitt V, Josey S A, Gille S T, Cerovečki I, Talley L D and Weller R A 2018 Episodic Southern Ocean heat loss and its mixed layer impacts revealed by the farthest south multiyear surface flux mooring *Geophys. Res. Lett.* **45** 5002–10

Scambos T and Stammerjohn S (eds) 2019 Antarctica and the Southern Ocean [in "State of the Climate in 2018"] *Bull. Am. Meteorol. Soc.* **100** S169–88

Schneider D P and Reusch D B 2016 Antarctic and Southern Ocean surface temperatures in CMIP5 models in the context of the surface energy budget *J. Clim.* **29** 1689–716

Scott R C and Lubin D 2016 Unique manifestations of mixed-phase cloud microphysics over Ross Island and the Ross Ice Shelf, Antarctica *Geophys. Res. Lett.* **43** 2936–45

Scott R C, Lubin D, Vogelmann A M and Kato S 2017 West Antarctic Ice Sheet cloud cover and surface radiation budget from NASA A-Train satellites *J. Clim.* **30** 6151–70

Semtner A J 1976 A model for the thermodynamic growth of sea ice in numerical investigations of climate *J. Phys. Oceanogr.* **6** 379–89

Silber I, Verlinde J, Wang S-H, Bromwich D H, Fridlind A M, Cadeddu M, Eloranta E W and Flynn C J 2019 Cloud influence on ERA5 and AMPS surface downwelling longwave radiation biases in West Antarctica *J. Clim.* **32** 7935–49

Sun R, Subramanian A C, Miller A J, Mazloff M R, Hoteit I and Cornuelle B D 2019 SKRIPS v1.0: a regional coupled ocean–atmosphere modeling framework (MITgcm–WRF) using ESMF/NUOPC, description and preliminary results for the Red Sea *Geosci. Model Dev.* **12** 4221–44

Van Tricht K, Lhermitte S, Lenaerts J, Gorodetskaya I V, L'Ecuyer T S, Noël B, van den Broeke M R, Turner D D and van Lipzig N P M 2016 Clouds enhance Greenland ice sheet meltwater runoff *Nat. Commun.* **7** 10266

Vitart F *et al* 2017 The subseasonal to seasonal (S2S) prediction project database *Bull. Am. Meteorol. Soc.* **98** 163–73

Wang H, Klekociuk A R, French W J R, Alexander S P and Warner T A 2020 Measurements of cloud radiative effect across the Southern Ocean (43° S–79° S, 63° E–158° W) *Atmosphere* **11** 949

Zampieri L, Goessling H F and Jung T 2019 Predictability of Antarctic sea ice edge on subseasonal time scales *Geophys. Res. Lett.* **46** 9719–27

Zou X, Bromwich D H, Montenegro A, Wang S and Bai L 2021 Major surface melting over the Ross Ice Shelf part II: surface energy balance *Q. J. R. Meteorol. Soc.* **147** 2895–916